Exploring the sensitivity of extreme event attribution ~~by~~ of two recent extreme weather events in Sweden using long-running meteorological observations

Erik Holmgren[1,2] and Erik Kjellström[1,3]

[1]Rossby Centre, Swedish Meteorological and Hydrological Institute, Norrköping, Sweden
[2]Division of Geoscience and Remote Sensing, Department of Space, Earth and Environment, Chalmers University of Technology, Gothenburg, Sweden
[3]Department of Meteorology and Bolin Centre for climate research, Stockholm University, Stockholm, Sweden

Correspondence: Erik Holmgren (erik.holmgren@chalmers.se)

Abstract. Despite a growing interest in extreme event attribution, attributing individual weather events remains difficult and uncertain. We have explored extreme event attribution by comparing ~~a widely adopted~~ the method for probabilistic extreme event attribution ~~to a more analogue approach~~ employed at World Weather Attribution[1], presented in Philip et al. (2020, WWA-method), to an approach solely using pre-industrial and current observations (PI-method), utilising the extensive, and long-running, network of meteorological observations available in Sweden. ~~The~~ With the long observational records~~enabled us~~, the PI-method is used to calculate the change in probability for two recent extreme events in Sweden without relying on the correlation to the global mean surface temperature ~~, as is usually done in the reference method.~~ (GMST). Our results indicate that the two methods generally agree ~~on the sign of attribution~~ for an event based on daily maximum temperatures. However, the ~~reference method~~ WWA-method results in a weaker indication of attribution compared to the ~~observations~~PI-method, where 12 out of 15 stations indicate a stronger attribution than found by the ~~reference method~~WWA-method. On the other hand, for a recent extreme precipitation event, the ~~reference method~~ WWA-method results in a stronger indication of attribution compared to the ~~observations~~PI-method. For this event, only two out of ten stations assessed in the PI-method exhibited results similar to the ~~reference method.~~ WWA-method. Based on the results, we conclude that at least 1 out of 2 of every heat wave similar to the summer of 2018 can be attributed to climate change. For the extreme precipitation event in Gävle in 2021, the large variations within, and between, the two methods make it difficult to draw any conclusions regarding the attribution of the event.

1 Introduction

Anthropogenic greenhouse gases are the main drivers of the observed increases in global temperatures during the 20th century (IPCC, 2021; Eyring et al., 2021). Even though the global warming is accompanied by a notable increase in the intensity, and frequency, of local extreme temperature and precipitation events (Trenberth, 2011; Seneviratne et al., 2021), linking individual extreme weather events to anthropogenic emissions remains a challenge.

[1]https://www.worldweatherattribution.org

Extreme weather events typically display unusual meteorological properties, cause severe effects on society, or occur relatively infrequently. However, the frequency and intensity of many of today's extreme events are expected to change with the ongoing changes of the global climate. For ~~some types of events~~ extreme events such as hurricanes (Holland and Bruyère, 2014) and heat waves (Wilcke et al., 2020), changes in their climatology have already been observed~~(e.g. Holland and Bruyère, 2014; Wilcke et al., . Extreme~~ . Furthermore, extreme weather, and its consequences, have often already been experienced, which makes it particularly interesting ~~. A popular question to ask~~ to scientists and the public alike. Hence, a question often asked is if any specific, especially intense, weather event was caused by ~~changes in the climate, and more specifically anthropogenic changes~~anthropogenic changes to the climate.

The relatively novel field of extreme event attribution (EEA) arose out of the need to try to answer questions like this. EEA is a collection of methods used to investigate if an extreme event can be attributed to any one forcing, such as anthropogenic climate change (e.g. Stott et al., 2016; van Oldenborgh et al., 2021). The last decade has seen a rapid increase in both the number of publications and general interest of EEA studies. A notable example is the BAMS special issue *Explaining Extreme Events* (e.g. Herring et al., 2022), which has been published annually since 2011. Olsson et al. (2022) argues that the increasing interest in EEA is connected to the ongoing development of the framework for Loss and Damages (L&D), where the attribution of single events could become a useful tool (Parker et al., 2015). The possible use of EEA in future L&D programs, combined with the increasing societal interest in extreme weather events, makes the exploration and evaluation of the suggested methods both compelling and important.

There are several approaches to EEA, where two of the more common ones are the risk-based approach and the storyline approach. In the risk-based approach, as described in e.g. Stott et al. (2016), the question of attribution is framed as probabilistic: *How has forcing x changed the likelihood of event y?* Here, it is the change in risk that an event occurs that is attributed to the changed forcing, rather than the event itself. This circumvents the otherwise difficult question of investigating the causal relationships of an extreme weather event. The storyline approach (e.g. Hoerling et al., 2013) instead focuses on the underlying physical processes in combination with the stochastic nature of an event. It tries to quantify the ~~role~~ effects of natural variability and forcings, such as increased greenhouse gases, sea surface temperature (SST) and soil moisture, had on the event. Due to these differences, EEA studies conducted on the same event, e.g. the Russian Heatwave in 2010, employing different methods, can appear to have reached contrasting conclusions (e.g. Dole et al., 2011; Rahmstorf and Coumou, 2011), even if both studies turned out to be compatible (Otto et al., 2012). Similarly, the use of different datasets can affect the outcome of an attribution study.

~~Data~~ To represent a climate that is not influenced by anthropogenic activities, the pre-industrial climate can be used as a proxy. However, data representing the pre-industrial reference period is scarce and often not available. Instead, it is possible to make use of the differences between current and historic conditions in the global mean surface temperature (GMST) to ~~shift, or scale,~~ adjust a distribution of the variable describing the event ~~(See 2.2)~~in today's climate, and in this way represent the pre-industrial climate ~~. These relationships are generally well-defined at global scales. Regionally, however, there are many factors influencing how changes in the global climate propagate and affect the local climate (Doblas-Reyes et al., 2021).~~ (Philip et al. 2020, See 2.2). This will be referred to as the WWA-method.

The last decade has seen a rapid increase in both the number of publications and general interest of EEA studies. A notable example is the BAMS special issue *Explaining Extreme Events* (e.g. Herring et al., 2022), which has been published annually since 2011. Olsson et al. (2022) argues that the increasing interest in EEA is connected to the ongoing development of the framework for Loss and Damages (L&D), where the attribution of single events could become a useful tool (Parker et al., 2015) . The possible use of EEA in future L&D programs, combined with the increasing societal interest in extreme weather events, makes the exploration and evaluation of the suggested methods both compelling and important.

One particularly interesting aspect of the reference method for probabilistic attribution WWA-method is the assumption of a linear relationship between GMST and the variable describing the event, and how this is used to represent the pre-industrial climate. However, this linear relationship will likely not capture other factors affecting the local response to global changesThese relationships are generally well-defined at global scales. However, regionally, there are many factors influencing how changes in the global climate propagate and affect the local climate (Doblas-Reyes et al., 2021), and the global linear relationship to GMST is unlikely to capture these. Hence, any local effects will not be included in likely be missing from the representation of the pre-industrial period, since it solely relies on how well the variable correlates to the GMST. . In turn, this could affect the outcome of an attribution study, where results stem from the difference in probability during the pre-industrial period and the recent past.

We aim to explore the proficiency of shifting, and scaling, adjusting the climate by GMST in the context of extreme event attribution in the simplest way possible: by comparing it to the results of the WWA-method to the results of a comparison between pre-industrial and current conditions based on observations. To achieve this, we will use the long-running observational network in Sweden to investigate two of the most notable extreme events in Sweden during the recent years: the particularly warm summer of 2018, in this study focused on southern Sweden, and the heavy precipitation event hitting impacting the Swedish city Gävle in August 2021. The heatwaves during the summer of 2018 have been featured in multiple recent studies (Leach et al., 2020; Yiou et al., 2020; Wilcke et al., 2020). Contrastingly, while the precipitation event in Gävle was heavily featured in the media and has been examined by the Swedish meteorological and hydrological institute (SMHI), studies focusing on the attribution of the event are lacking. By including the two events in the same study, we also aim to highlight the differences with the attribution of events based on different meteorological variables (temperature and precipitation).

For both of these events, we will perform two sets of attribution studies, employing different methods , and compare their resultsemploy two different methods for EEA. The first analysis is based on the using the method from the rapid attribution framework from Philip et al. (2020)(Philip et al., 2020, WWA-method), while the second analysis will instead make use of directly compare the pre-industrial and current period using data from several stations with observational records covering both the current and a pre-industrial periodlong observational records, thus not adding the dependency on the GMST (referred to as the PI-method).

2 ~~Method~~Data and Methods

In this study, we will employ parts of the rapid attribution framework from ~~Philip et al. (2020)~~ (Philip et al., 2020, WWA-method) to investigate the possible attribution of two recent events in Sweden: The warm summer of 2018 and the heavy precipitation event in Gävle on the 17-18th of August 2021. Alongside this more commonly used attribution method, we will ~~also~~ perform an analysis based on long-running series of meteorological observations (PI-method).

2.1 ~~Probabilistic extreme~~ Gridded datasets and event ~~attribution~~definitions

We defined two different domains to represent the events: one for the heat wave in the summer of 2018 and one for the heavy precipitation event in Gävle 2021 (Fig. 1). The domain for the summer of 2018 covers the mainland of Sweden south of 60°N, whereas the domain for the Gävle event covers between 59°N and 63°N, and east of 13.5°E.

We used the following gridded datasets: GridClim (Andersson et al., 2021), PTHBV (Gävle only, Johansson and Chen, 2005; Alexandersso , E-OBS (Cornes et al., 2018), and ERA5 (Hersbach et al., 2020). Additionally, we also used a bias adjusted (Berg et al., 2022), 66-member, version of the Euro-CORDEX ensemble (Coppola et al., 2021; Jacob et al., 2014), as described in Kjellström et al. (2022) . GridClim, E-OBS, ERA5, and the CORDEX ensemble all provided data until the end of 2018, while PTHBV covered up until the end of 2021. To assess how well the individual members of the CORDEX ensemble represented observations, we computed the four metrics used in Bayerisches Landesamt für Umwelt (2020) between 1989 and 2018 for the respective domains, using GridClim as the reference dataset. For all datasets, grid points outside the Swedish mainland were masked.

For each dataset, we used 30 years of daily data to define the period representing the recent past. In the context of analysing return times of extreme events, 30 years is a rather short period, and using a longer time series is generally desirable. However, for this study, we chose a shorter period for two reasons. Firstly, we wanted to keep the period defining the climate of the recent past the same for both methods. Secondly, we wanted the period defining the current climate to be relatively stationary, limiting the climate signal from local changes in e.g. aerosol emissions.

For the summer of 2018 event, we used the daily maximum temperatures between 1989 and 2018, and we used the daily precipitation flux between 1991 and 2021 for the Gävle event. For both the events, we chose to include the events under investigation in the time series used in the following analysis.

We used two climate indicators to describe the events: the number of days with maximum temperature ≥ 25°C (txge25) for the summer of 2018 event, and the maximum 1-day precipitation (rx1day) for the Gävle 2021 event. The summer 2018 in Sweden was characterized by several long-lasting high-pressure weather situations. This led to a record number of warm days, which was one of the unique features of that summer (Wilcke et al., 2020). Consequently, we define our event by using the txge25 index since that better reflects the longevity of the event rather than capturing the intensity in any single day or short period. August 2021 came with large amounts of precipitation in southern Sweden. The most intense event resulted in more than 100 mm in 24 hours between the 17th and 18th of August for a large area close to the city of Gävle, which was highly impacted by the resulting flooding. For a relatively short-lived event like this, we chose to define our event by using the rx1day index.

We calculated the indicators using the software Climix (Zimmermann et al., 2023). For the summer 2018 event, only days within the period from May to August (MJJA) were used to calculate txge25, while rx1day was calculated over the entire year. Furthermore, for the index describing the summer 2018 event, we calculated the domain average for each year. Since heavy precipitation events are generally more localised compared to heat waves, we instead opted to calculate the annual domain maxima for the index describing the Gävle 2021 event.

2.2 Attribution using the WWA-method

The rapid attribution framework from Philip et al. (2020) is a risk-based approach to attribution. It consists of steps outlining the preparations, analysis, and communication of an attribution study. In the following section, we will describe parts of the statistical method outlined in the framework.

The final result of a probabilistic attribution study is the probability ratio (PR)

$$\mathrm{PR} = \frac{p_1}{p_0}, \tag{1}$$

or fraction of attributable risk (FAR)

$$\mathrm{FAR} = 1 - \frac{p_0}{p_1} = 1 - \frac{1}{\mathrm{PR}}, \tag{2}$$

where p_1 and p_0 are the probabilities ~~for the event~~ of observing an event of an equal, or greater, magnitude than the event threshold in the factual (current climate) and counterfactual (pre-industrial climate) worlds (see Fig. 2). PR and FAR are interchangeable, and which one to use depends on how the results will be presented. PR is interpreted as how many times more likely (or unlikely if <1) an event with the same magnitude has become. FAR instead describes ~~how large fraction~~ the proportion of events of the same, or greater, magnitude that can be attributed to the changed forcing. For instance, if the PR of an event is 2, the interpretation would be that it has become twice as likely. On the other hand, the interpretation of the corresponding FAR$= 0.5$ is that half of the occurrences of similar events can be attributed to the changed forcing.

To calculate p_1 and p_0, ideally long observational datasets and climate model output, which contain periods that represent both the current and pre-industrial climate, should be used. The exceedance probability of a class of events, in either of the two periods, can then be sampled from the continuous density function (CDF) of a theoretical distribution fit to data ~~corresponding to that~~ representing the period (see Fig. 2). In most cases, data describing the current climate is readily available, either from observations, reanalysis products, or models, and retrieving p_1 is relatively trivial.

Computing p_0 requires data ~~of~~ covering the pre-industrial period. Unfortunately, continuous observations with good spatial coverage from ~~these~~ pre-industrial times are rare. ~~One~~ Instead, one option is to use the output of climate models. For instance, General Circulation Models (GCMs) part of the Coupled Model Intercomparison Project (CMIP, Eyring et al. 2016) have a pre-industrial control run which could be used to represent the pre-industrial climate in attribution studies. ~~A second option is to use fixed forcing GCM runs, with for instance prescribed sea surface temperature. However, the resolution of GCMs is~~ A drawback of the GCMs is that their resolution is generally too low to properly represent many extreme weather events. The increased resolution of regional climate models (RCMs), for instance members of the Coordinated Regional Climate

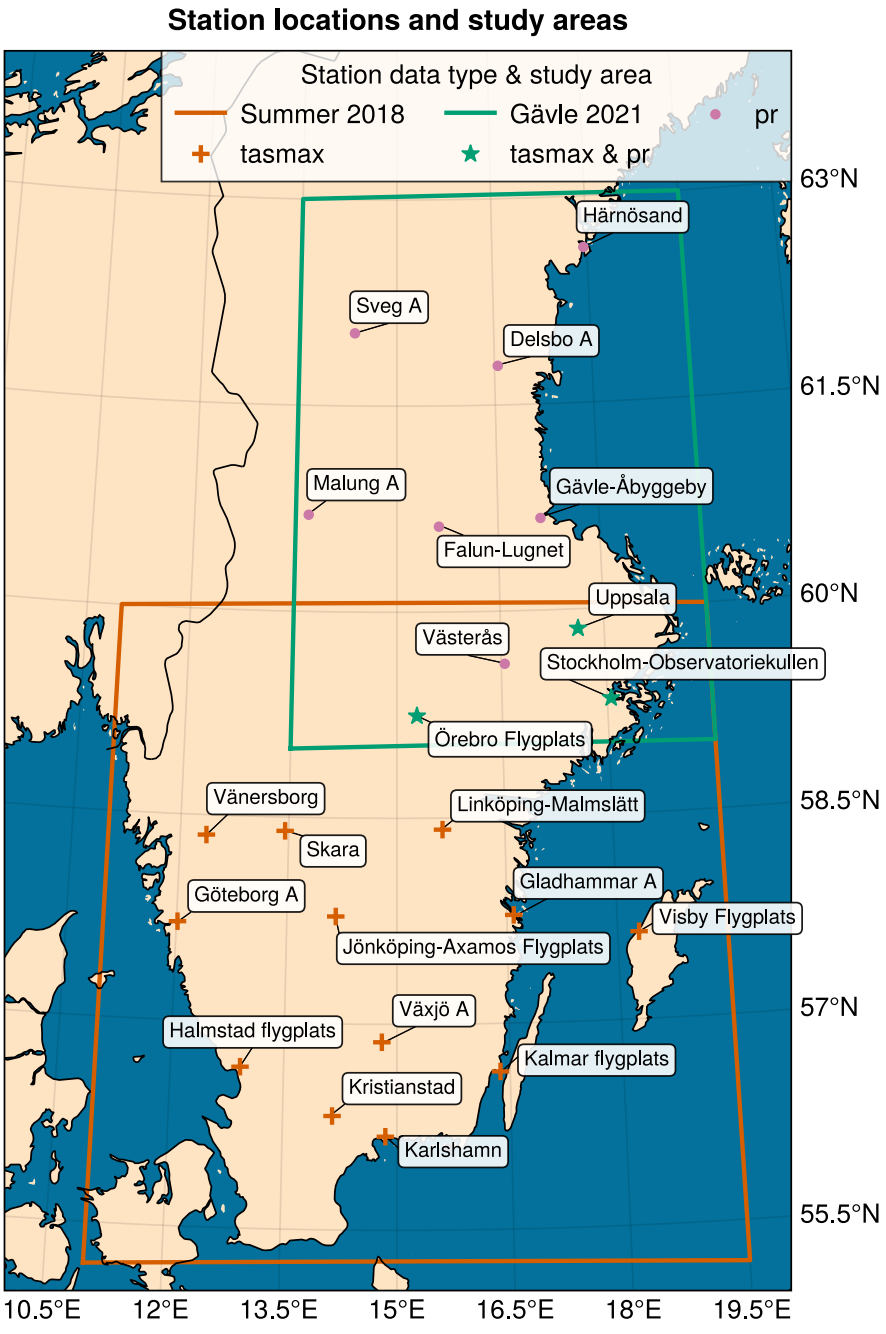

Figure 1. Domain outlines and the locations of stations used in the study. Purple dots visualise stations used only for precipitation data, the orange plus are used for temperature data, and green stars show stations used for both precipitation and temperature. Coloured boxes show the outlines for the regions used in selection of the gridded data.

Downscaling Experiment (CORDEX, Jones et al. 2011) ensemble, ~~does enable the models to better represent~~ enables better representation of extreme weather events. However, the high resolution runs completed in CORDEX traditionally do not include ~~a~~ the pre-industrial control period, and thus only cover a period from the middle of the 20th century and forward.

A third option ~~for~~ used to represent the pre-industrial climate, and what is used in this and many other attribution studies, is to shift, or scale, the distribution that represents the current climate. This relies on the assumption that the variable used to describe the event shifts or scales with a forcing that has a known climate change signal and historical record. An example of this is the global mean surface temperature (GMST), commonly used as a key indicator of climate change (e.g. Gulev et al., 2021).

~~A theoretical distribution, e.g. the GEV distribution, can be described by three parameters: the location , scale, σ, and shape, ξ. To shift a distribution according to its relationship with GMST, μ~~ The location μ of a distribution is shifted following

$$\mu = \mu_0 + \beta\Delta T. \tag{3}$$

Here μ_0 is the initial location, β is the coefficient of the linear regression between the variable and GMST, and ΔT is the change in GMST between the current and pre-industrial period. ~~σ and ξ are left unchanged.~~ If the variable is instead assumed to scale with GMST, which is the case for precipitation, μ and the standard deviation σ are changed following

$$\mu = \mu_0 \exp(\beta\Delta T/\mu_0) \tag{4}$$

and

$$\sigma = \sigma_0 \exp(\beta\Delta T/\sigma_0). \tag{5}$$

Either of these approaches will result in a distribution that represents the pre-industrial climate, where the CDF can be sampled to retrieve p_0 (see Fig. 2).

~~In this study, we defined two domains used for the analysis of the events, one for the heat wave in the summer of 2018 and one for the heavy precipitation event in Gävle 2021 (Fig. 1). The summer 2018 domain covers the mainland of Sweden south of 60°N. For the Gävle event we used a region between 59°N and 63°N, and east of 13.5°E. We extracted 30 years of daily data for the two events, forming the reference periods used to retrieve p_1. For the summer of 2018 event, this consisted of daily maximum temperatures between 1989 and 2018, while for the Gävle event, daily precipitation flux between 1991 and 2021 was analysed.~~

~~We used the following gridded datasets: GridClim (Andersson et al., 2021), PTHBV (only for Gävle) (Johansson and Chen, 2005; Alexand , E-OBS (Cornes et al., 2018), and ERA5 (Hersbach et al., 2020). Additionally, we also used a bias adjusted (Berg et al., 2022), 66-member, version of the Euro-CORDEX ensemble (Coppola et al., 2021; Jacob et al., 2014), as described in Kjellström et al. (2022) . GridClim, E-OBS, ERA5, and the CORDEX ensemble all provided data until the end of 2018, while PTHBV covered up until the end of 2021. To assess how well the individual members of the CORDEX ensemble represented observations, we computed the same four metrics as used in Bayerisches Landesamt für Umwelt (2020), between 1989 and 2018 over Sweden, using GridClim as the reference dataset. For all datasets grid points outside the Swedish mainland were masked. Following~~

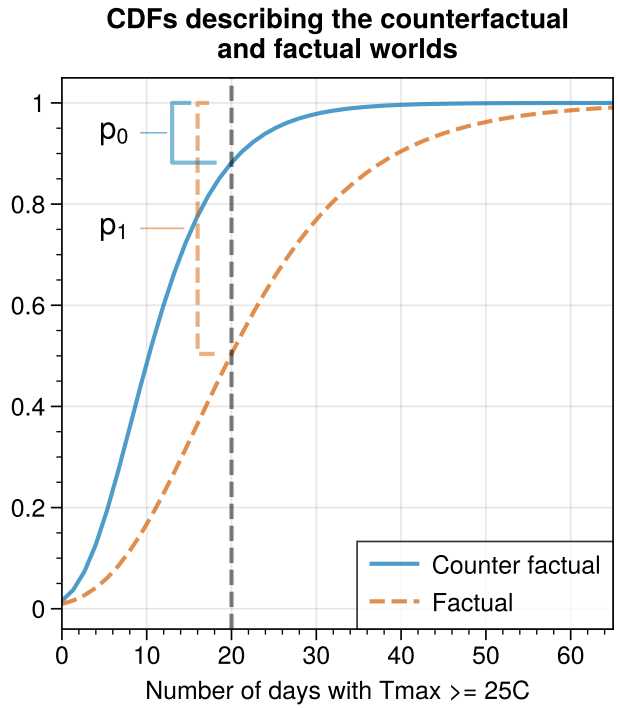

Figure 2. Conceptual image describing the relationship between CDF and probability. Here, the two CDFs describe the distributions of the annual number of days with Tmax $\geq 25°$C in a factual and counterfactual world. An event threshold of 20 days is indicated by the grey vertical line. The corresponding event probabilities p_1 and p_0 are visualised as ~~bracketed annotations~~square brackets. p_1 is in this case larger than p_0, which indicates that a summer with 20 days or more with a daily maximum temperature $\geq 25°$C is more likely in the factual world.

~~this , we calculated climate indicators, further described in section 2.1. For the index describing the summer 2018 event, we calculated the domain average for each year. Since heavy precipitation events are generally more localised compared to heat waves, we instead opted to calculate the annual domain maxima for the Gävle 2021 event.~~

~~Following Philip et al. (2020), we computed the~~ We computed the linear regression between the 4-year ~~rolling mean GMST (Hansen et al., 2010) and the annual time series of each index~~rolling mean GMST (Hansen et al., 2010) and the 30-year annual time series of each index. This differs slightly from (Philip et al., 2020), where they estimate β, μ, and σ directly from eq. 3, 4 and 5. However, since the distributions used in this analysis were found to be invariant to linear transformations (not shown), this does not affect the outcome. For the CORDEX ensemble, the regression coefficient of each ensemble member was used as an additional quality control, where we removed any ~~member with a regression coefficient outside~~ ensemble member where the regression coefficient exceeded the 95% confidence interval of the regression in the reference dataset (GridClim). For all datasets, we used the regression coefficients to detrend the index-series of the current climate. For each index series, we then fit and evaluated a number of common extreme value distributions and selected one for further analysis (see sec. 2.4). We then used the regression coefficients (β) to respectively shift and scale the index distributions describing the summer of

2018 and Gävle 2021 events according to eq. 3, 4 and 5. For each dataset, the distribution of the current climate and the pre-industrial (shifted/scaled) distribution formed a pair from which p_1 and p_0 could be retrieved and used to calculate FAR/PR (Eq. 1 & 2). The threshold used for the summer of 2018 event was based on the 2018 domain average txge25 in the GridClim product, whereas we used the 2021 domain maximum rx1day in PTHBV for the Gävle 2021 event. For the gridded observations (GridClim, PTHBV, E-OBS, ERA5) we calculated confidence intervals with a bootstrap of randomly re-sampling the 30-year index-series and performing the previous steps 1000 times. For the CORDEX data, instead of bootstrapping the confidence intervals, FAR from each ensemble member was used to form the distribution from which the confidence intervals could be retrieved.

2.3 Attribution using ~~observations~~the PI-method

As an alternative to the ~~more common method outlined above~~WWA-method, we performed an attribution analysis employing several stations with long observational records of daily data. ~~To begin~~First, we employed a set of station merges commonly used at SMHI to extend and fill the gaps in the observational records for temperature and precipitation (e.g. Joelsson et al., 2022). This merges nearby stations which are assumed to be representative of the same geographic location but have different temporal coverage. The ~~merged stations were used to select two sets of stations, one for each of the investigated events. The~~ observational records were checked for missing values and a station missing $\geq 15\%$ of the days in the investigated period, during at least one year, were flagged in the subsequent analysis.

For each event, we selected all stations located inside the domain on the Swedish mainland and the island Gotland (Fig. 1). For ~~the station data we calculated the same climate indices as was done for the gridded datasets (see 2.1). Following the index calculations, we further refined the station selection by requiring each station to provide a continuous 30-year period for both the historic and current climate. For both~~ both events, the ~~historic~~ pre-industrial period was defined as ~~the years~~ 1882 to 1911. This represents a period largely unaffected by anthropogenic climate change~~and~~ , yet it is relatively well covered in the observational records. The current climate period for the summer of 2018 was defined ~~by the years~~ as 1989 to 2018, ~~while~~ and 1992 to 2021 for the Gävle 2021 event~~as the years 1992 to 2021.~~ . We calculated the same climate indices as for the gridded datasets (see 2.1) for each station. Following the index calculations, we further refined the station selection by requiring each station to provide a continuous 30-year period for both the pre-industrial and current period. The selection procedure resulted in 15 stations for the 2018 event and 10 stations for the 2021 event. The locations and names of these stations are shown in ~~figure~~ Figure 1. We checked the two separate periods of each station data for stationarity using the Kwiatkowski-Phillips-Schmidt-Shin (KPSS) and Augmented Dickey-Fuller (ADF) tests (See Appendix A). ~~Locations of stations employed in this study. Purple dots visualise stations used only for precipitation data, the orange plus are used for temperature data, and green stars show stations used for both precipitation and temperature. Coloured boxes show the outlines for the regions used in selection of the gridded data.~~

The two periods representing the ~~historic~~ pre-industrial climate and that of the recent past were then used to calculate PR and FAR following eq. 1 and 2, in the same way as done in the probabilistic event attribution (Section 2.2). Here, the threshold for the summer of 2018 was set to the 2018 station averaged txge25, while the ~~2021~~ value of rx1day ~~from~~ for Gävle-Åbyggeby

in 2021 was used as a threshold for the Gävle event. Furthermore, we also ~~compared these results to those obtained by either shifting or scaling the distribution representing the current period~~ computed FAR for each station using the WWA-method.

2.4 ~~Climate indicators~~

~~We used two climate indicators to describe the events: the number of days with maximum temperature $\geq 25°C$ (~~In this study, we have used the txge25 ~~) for the summer~~ indicator to quantify the warm summer of 2018. This is very similar to the more common indicator su (often referred to as summer days), defined as the number of days when $T_{max} > 25°C$. For model data, where the number of reported decimals are plenty, this choice has little to no consequence. For observations, however, and specifically from manual historical records, there is a notable difference between counting days when $\mathrm{tasmax} > 25°C$ and where $\mathrm{tasmax} \geq 25°C$. The reason is that decimal points were not prioritised in early observational practices, e.g. a thermometer displaying 25.4°C may have been recorded as 25°C. In our case, the average median FAR for the summer of 2018 ~~event, and the maximum 1-day precipitation (rx1day)for the Gävle 2021 event. We calculated the indicators using the software Climix (Zimmermann et al., 2023). For the summer 2018~~ event ~~, only days within the period from May to August (MJJA) were used to calculate the indices, while rx1day was calculated over the entire year.~~ using the PI-method decreased from ~ 0.65 for the su index to ~ 0.48 for the txge25 index, an indication that using the former index results in an underestimation of warm days in the pre-industrial period.

2.4 A note on distributions

In this study, we used the python package SciPy (Virtanen et al., 2020) to fit, evaluate and sample the distributions used to represent the data. There are multiple distributions suitable to represent extreme distributions, for instance GEV, Gaussian, GPD or Gumbel. We refer to Philip et al. (2020) for further details on the selection of distributions. It is common practice to use a goodness of fit test, such as the Kolmogorov-Smirnov test (KS-test), to evaluate the suitability of the different distributions to represent the data. However, we have found that relying solely on the KS-test for selecting the appropriate distribution insufficient. Most notably, while the GEV distribution tends to show the highest performance in the KS-test, it often results in division by zero errors in Eq. 1 for very high quantiles. The right-skewed Gumbel distribution does not lead to the same division by zero errors, while it still shows good performance in the KS-test. A theoretical explanation for this is that the GEV distribution has a finite upper bound due to its negative shape parameter, which can result in events becoming theoretically impossible. The Gumbel distribution, on the other hand, has no upper bound since its shape parameter is fixed at zero, and events are never theoretically impossible. Because of this and the confirmation from the KS-test that it could represent our data, we opted to use the right-skewed Gumbel distribution for all probability estimations in this analysis.

3 Results and Discussion

3.1 Summer of 2018

Almost all the stations employed in the analysis (Fig. 1) recorded ≥ 50 days with daily maximum temperatures $\geq 25°C$ (summer days) during the summer of 2018 (Fig A2), here defined as May to August (MJJA). There are only a few stations where this is not, by some margin, the highest number of summer days recorded between 1989-2018. Between 1882-1911, there are no years that equals the number of summer days in 2018 among any of the stations (Fig. A3).

Histograms, along with the distributions, generally show a positive difference between the distributions of the current and ~~historic climate for~~ the pre-industrial climate for txge25 ~~index~~ (Fig. 3). Consequently, the PI-method generally yields positive values for FAR, with medians > 0.8 for most of the stations (Fig. 3). It is only Kristianstad, Karlshamn and Linköping-Malmslätt (LM) ~~exhibit the smallest difference between the two periods. The median FAR for LM is -3.4 while most other stations exhibit a median FAR > 0.8 (Fig. 3).~~ that exhibit FAR medians < 0. Here, a FAR ≤ 0 implies that no occurrences of an event of similar, or greater, magnitude can be attributed to the changed forcing. Furthermore, there are no spatial patterns over southernmost Sweden that could explain the negative FAR of LM and Karlshamn (Fig. 4).

~~The station-averaged FAR for the txge25 index has a median of 0.50~~ Taking the average of the stations included in the PI-method for the summer of 2018 event gives a median FAR ~ 0.50 with the 5th percentile (~~P~~Q_5) $\sim$ -0.78 (Fig. 5). ~~This further highlights~~ The FAR distributions (Fig. 5) further highlight the anomalous behaviour of LM, where neighbouring stations Skara, Gladhammar A and Örebro Flygplats (see Fig. 1 & 4) display FAR distributions centred ≥ 0.75. For ~~the adjusted station average~~ an adjusted average of the PI-method (Fig. 5), where Karlshamn, Kristianstad and LM are excluded, the median FAR ~ 0.78, and ~~P~~$Q_5 > 0.1$.

The deviating results of ~~the excluded~~ these two stations are likely not the result of a local response to changes in ~~the~~ climate. Instead, it is more likely a result of the station merging. In some cases, merging implies that the station is moved to a new location. For LM, the station was moved a few kilometres west from central Linköping to the airfield at Malmslätt in 1943. Since temperatures are generally higher in urbanised areas due to the urban heat island (Rizwan et al., 2008), moving the station to a more rural area could introduce erroneous trends to the series (e.g. Tuomenvirta, 2001; Dienst et al., 2017). On the other hand, Karlshamn is an example of stations ~~which~~ that provides a continuous observational record without merges or changes in location. Here, the implementation of thermometer screens during the 20th century, which generally results in reduced recorded temperatures, could be a part of the explanation.

These are examples of inhomogeneities in the observational record that makes the investigation of trends and climate change difficult. Ideally, when working with signals of climate change in observational data, the data should first be homogenised, however, for daily data this is currently not available in Sweden. Joelsson et al. (2022) presents monthly averages of the 2-metre temperature in Sweden from 1860, based on homogenised data from a high number of stations. The stations used in this study are a subset of the stations used in Joelsson et al. (2022). Since this study makes use of daily temperatures, we ~~can not~~ cannot directly utilise their results. However, their findings can help to further evaluate our results. In general, they found the required temperature corrections to be negative, with larger corrections during summers at the end of the 19th, and beginning

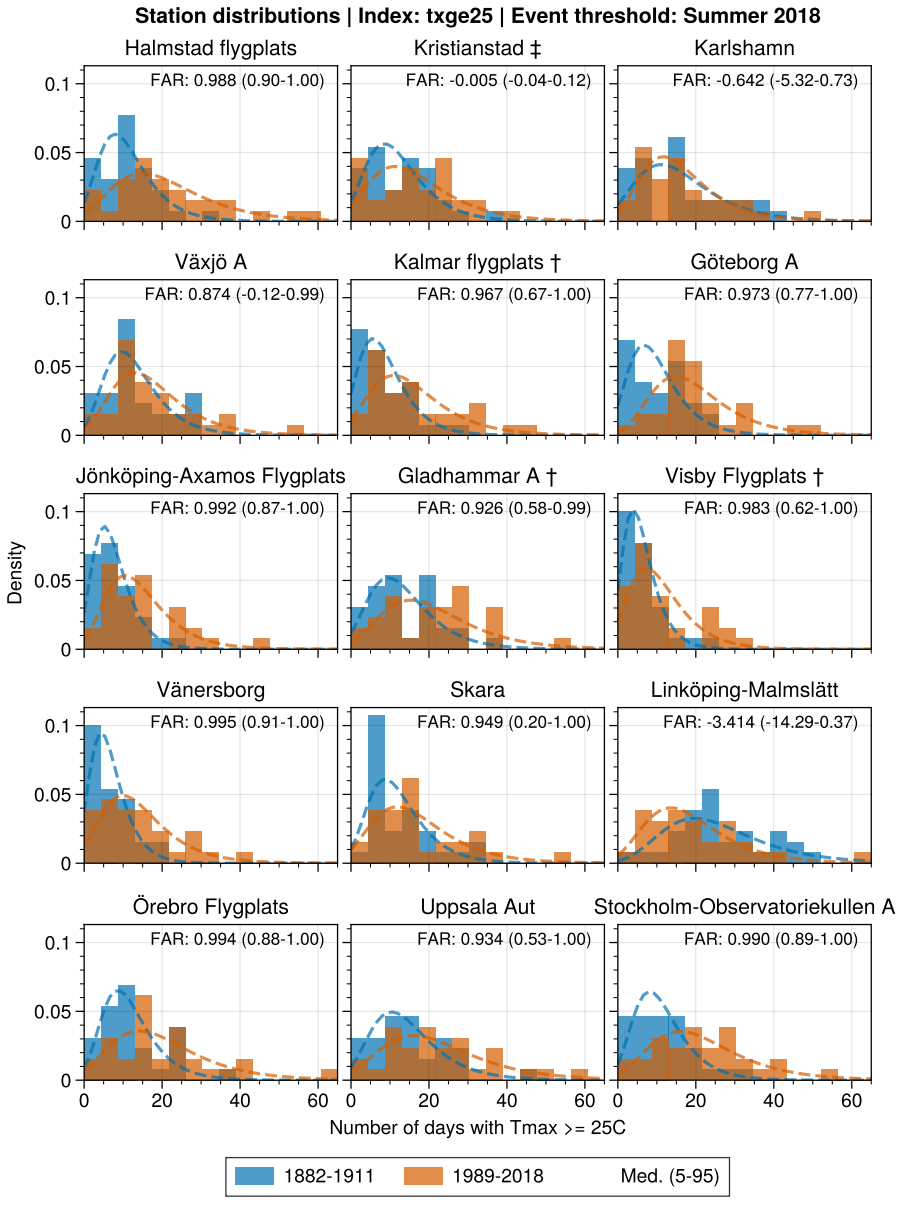

Figure 3. Histograms of the txge25 index for the periods ~~1882-1992~~ 1882-1911 and 1989-2018. Dashed lines show the pdf of the Gumbel distribution fit to each period. ~~2018 is used as a threshold for FAR for each station.~~ † indicate that at least one year miss 15% of the days in the ~~historic~~ pre-industrial period. ‡ is the equivalent for the current period.

of the 20th, century. For instance, their analysis indicates a homogeneity break in maximum temperature during 1890 for the station of Karlshamn, which coincides with the pronounced shift towards lower numbers in txge25 in Fig. A3. This implies

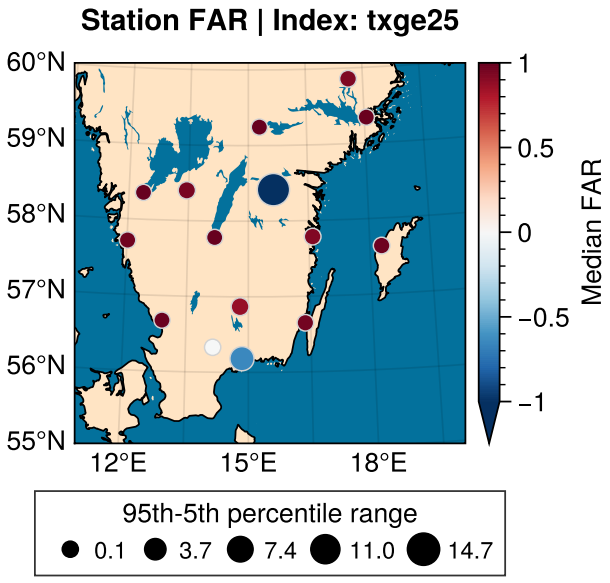

Figure 4. ~~Station locations~~FAR for the summer of 2018 at the stations used in the study. ~~Marker~~ The marker colour ~~shows~~ represents the median FAR, while the marker size shows the uncertainty range in FAR as the range between the 95th ~~to~~ and 5th percentile~~range~~.

that the estimated event probabilities during the pre-industrial period in this study are likely too high, which in turn results in an underestimation of FAR.

The analysis ~~of the gridded data products, using shifted distributions,~~ using the WWA-method, exhibits FAR similar, albeit lower, to ~~that of the station data~~ FAR estimated using the PI-method (Bottom five bars, ~~fig~~Fig. 5). The FAR distributions for GridClim, E-OBS and ERA5 all exhibit a median of 0.4-0.6 and a low spread, and with 5th percentiles well above 0. The CORDEX ensemble FAR distribution, here with 62 members, shows a higher median (~ 0.8), ~~however it exhibits~~ albeit with a greater spread (~~P~~$Q_5 \sim -4$, ~~$P_{25} \sim 0.2$~~$Q_{95} \sim 0.99$) compared to the observational based products (~~P~~$Q_5 \sim -0.8$, ~~$P_{25} \sim 0.1$~~$Q_{95} \sim 0.9$). The ~~weighted average of the gridded products~~ grid average (Fig. 5) shows the average FAR distribution of the datasets used in the WWA-method. Here, the median FAR is lower compared to the adjusted station average of the PI-method, but uncertainty ranges overlap.

3.2 Gävle 2021

During the event on the 21st of August 2021, the station Gävle-Åbyggeby measured 121 mm of precipitation in 24 hours. This ~~corresponds to~~ is also the annual maximum one day precipitation (rx1day) at that station in 2021. In 2021, ~~no other station~~ none of the other assessed stations in the study area (Fig. 1) recorded a similar amount of precipitation in a single day. However, there are years in the recent past with annual daily maximums similar to the Gävle 2021 event, both in Gävle and at other

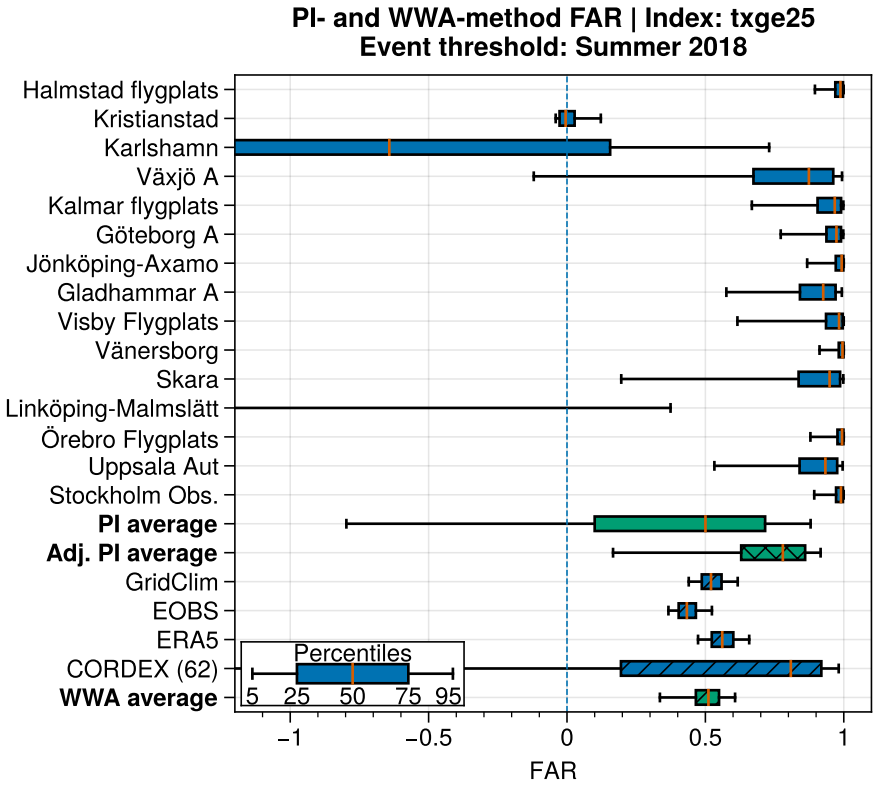

Figure 5. FAR synthesis for the summer of 2018, as described by the txge25 index during MJJA. ~~For station data, A~~ a bar visualise the ~~factual and counterfactual worlds are represented by observations from 1989-2018 and 1882-1911, respectively~~percentiles of the FAR distribution as described in the inset. Green bars denote ~~station/dataset~~ averages ~~. Hatched bars display results from gridded data products, whereas~~ of the two methods (PI & WWA). The green crossed bar shows the adjusted ~~station~~ average ~~. A bar visualise~~ for the ~~bootstrap distribution percentiles as described in~~ PI-method, whereas the ~~inset~~hatched bars (blue & green) display results from the WWA-method. Note that the x-axis is limited for increased readability.

stations (Fig. A4). In the ~~historic period there are only two~~ pre-industrial period there were only two recorded events, both in Härnösand, with similar magnitudes to the 2021 event (Fig. A5).

For an event like the heavy precipitation event in Gävle 2021, differences between the ~~historic~~ distributions of the pre-industrial and current climate are small at most of the 10 stations used to investigate the event (Fig. 6). ~~Some~~ There are a few stations (e.g. Gävle-Åbyggeby, Härnösand, Sveg A) that exhibit larger differences between the two periods, most notably in the tails of the distributions~~, between the two periods~~.

The FAR synthesis of the PI-method (Fig. 7) ~~displays~~ shows the large variability among the stations. Here, Uppsala is the only station where the confidence interval doesn't include 0, ~~P~~$Q_5 \sim 0.2$. ~~Looking~~ When looking at the median, however, Gävle-Åbyggeby, Sveg A, Uppsala, Västerås, and Örebro D all exhibit FAR > 0. The remaining stations (Falun-Lugnet, Härnösand,

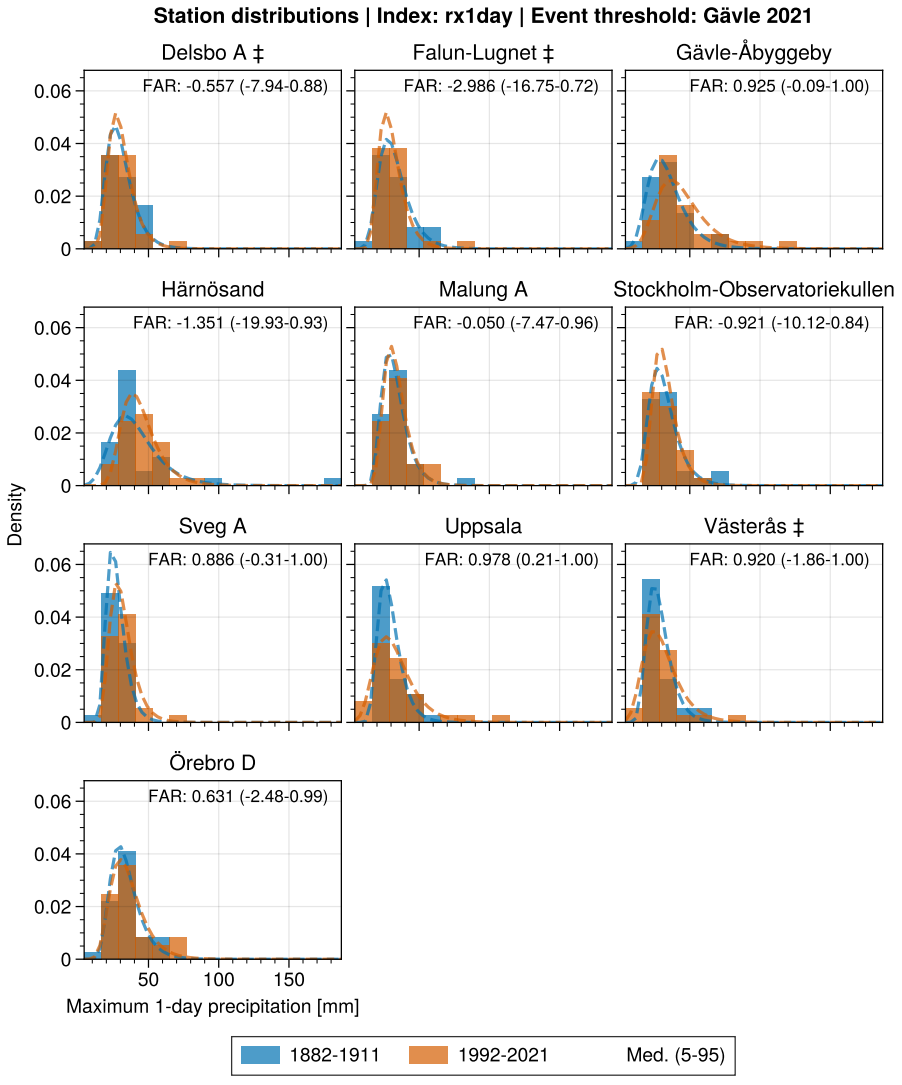

Figure 6. Histograms of ~~the~~ annual ~~maximum 1-day precipitation index~~ rx1day for periods ~~1882-1992~~ 1882-1911 and 1992-2021. Dashed lines show the pdf of the gumbel distribution fit to each period. ~~2018 is used as a threshold for FAR for each station. †~~ ‡ indicate that at least one year miss 15% of the days in the ~~historic period. ‡ is the equivalent for the~~ current period.

Malung A, Stockholm-Observatoriekullen) show a median FAR ≤ 0~~, which indicates that the event has become less likely~~. These differences are reflected by the large spread ~~exhibited by the station average in~~ and negative median ($Q_{50} \sim -0.2$) of the average of the stations used in the PI-method for the Gävle event (Fig. 7~~($P_{50} \sim -0.2$~~).

FAR distributions from the ~~gridded analysis of~~ WWA-method for the Gävle 2021 event are shown in the hatched bars in Fig. 7. PTHBV, GridClim, EOBS and CORDEX exhibit similar medians (0.78-0.98), ~~P~~and $Q_5 \geq 0.6$. ~~Results~~ The results from ERA5 does not match the other datasets, with a median FAR ~ -2.5 and ~~P~~$Q_{95} \sim -2$. We also ~~noted~~ note that ERA5 exhibits a

negative regression to GMST, as opposed to the other datasets where the regression is generally positive. A contributor to this could be the overall underestimation of rx1day in ERA5 found by Lavers et al. (2022). This requires further investigation, and we chose not to include ERA5 in the Grid Average FAR.

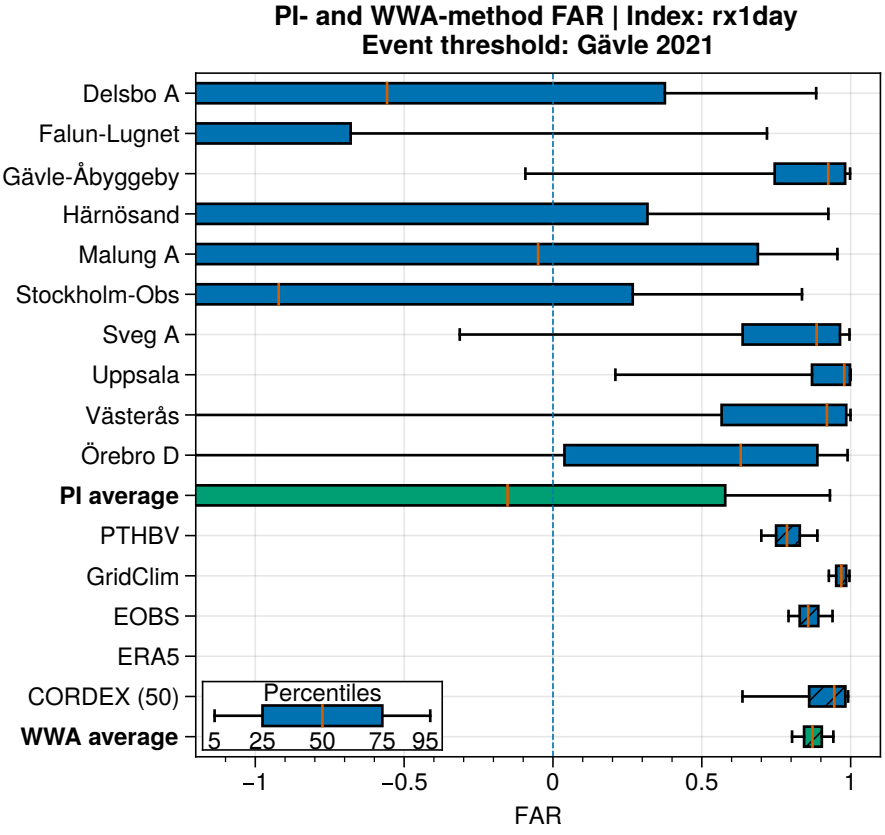

Figure 7. FAR synthesis for the heavy precipitation event in Gävle 2021 described by the annual maximum 1-day precipitation (rx1day). ~~The factual and counterfactual worlds are represented by station data from periods 1992-2021 and 1882-1911, respectively. The median station FAR for an event similar to Gävle 2021 is ~-0.2. Hatched bars display results from gridded data products.~~ A bar visualise the ~~bootstrap distribution~~ percentiles of the FAR distribution as described in the inset. Green bars denote averages of the two methods (PI & WWA). The green crossed bar shows the adjusted average for the PI-method, whereas the hatched bars (blue & green) display results from the WWA-method. Note that the x-axis is limited to -1 for readability. The ERA5 FAR distribution lies below this range and is not displayed.

~~There~~ For the Gävle event, there is some disagreement between the ~~station-based results and the results of the gridded analysis~~WWA-method and the PI-method. For stations such as Gävle-Åbyggeby, Sveg A, Uppsala, Västerås, and Örebro D, the median FAR derived by the PI-method is of the same magnitude as that of the ~~gridded analysis~~WWA-method. However, uncertainties are generally greater for the ~~station-based analysis, with lower~~ PI-method, and with 5th percentiles < 0 for multiple stations. Here, the difference in the magnitude of uncertainty between the two methods can likely be attributed to the

fact that gridded data typically does not represent extreme precipitation events as well as local observations, and thus has an overall lower variability. ~~Here it is worth remembering that all FAR distributions, from both gridded data and observations, are based on the same number of samples and bootstrap iterations.~~ Furthermore, the relatively short 30-year period used to represent the current climate further limits how accurately the gridded datasets can represent the variability. This results in a possibly over constrained distribution, which can lead to unrealistic estimates of FAR.

The question of homogeneity in the station data also applies to the precipitation measurements. During the later parts of the 20th century, many stations have been converted from manual to automatic operation in Sweden. Here, the placement of automatic stations were generally more exposed to wind compared to manual stations, where comparisons have shown that automatic ~~precipitation measurements are lower~~ measurements generally show less precipitation compared to those of manual stations (Alexandersson, 2003).

The two 30-year periods used to represent the pre-industrial (1882-1911) and the current (1992-2021) climate were found to be stationary at most of the stations (Fig. A5 & A4). Based on this, we decided not to detrend the station data. This also kept the following analysis (PI-method) closer to the actual observations, ~~removing any~~ not adding a dependence on regressions to e.g. GMST. Comparing the pre-industrial and current climate, most of the stations show distributions with very similar means (Fig. 6). In these cases, the results ~~will be~~ are more sensitive to the randomness of the bootstrap, resulting in the large uncertainties for some stations in Fig. 7.

3.3 ~~The effect of observational accuracy~~ Comparing the PI and ~~implications of correlating to GMST~~WWA methods

~~In this study, we used the txge25 indicator to quantify the warm summer of 2018. This is very similar to the more common indicator su (often referred to as summer days), defined as the number of days when $T_{max} > 25°C$. For model data, where~~ The long observational time series enables us to directly evaluate to what degree the two methods agree. This is presented as FAR distributions for the two events in Figs. 8 and 9. These are derived by applying both the PI-method and the WWA-method to the ~~number of reported decimals are plenty, this choice has little to no consequence. However, for observations, and specifically from manual historical records, there is a notable difference between counting days when $tasmax > 25°C$ and where $tasmax \geq 25°C$. The reason is that decimal points were not prioritised in early observational practices, e.g. a thermometer displaying 25.4°C was likely recorded as 25°C. In our case, the station averaged median FAR for the summer of~~ long-term observations.

The results clearly show that the two methods generally yield similar results for the summer of 2018 ~~event decreased from ~ 0.65 for the su index to ~ 0.48 for the~~ (Fig. 8), albeit with somewhat lower FAR numbers for the WWA-method compared to the PI-method. Likely, this is a result of the weak regression coefficient between the variable (txge25~~index, an indication that using the former index results in an underestimation of warm days in the pre-industrial period~~) and GMST (Fig. A1). There are two stations, Karlshamn and Linköping-Malmslätt, where the WWA-method results in a higher estimation of FAR compared to the PI-method. Interestingly, for both these stations, the WWA-method yields FAR distributions more aligned with the FAR (WWA & PI) of the other stations used in the analysis. Overall, this suggests that the WWA-method, even when applied to only

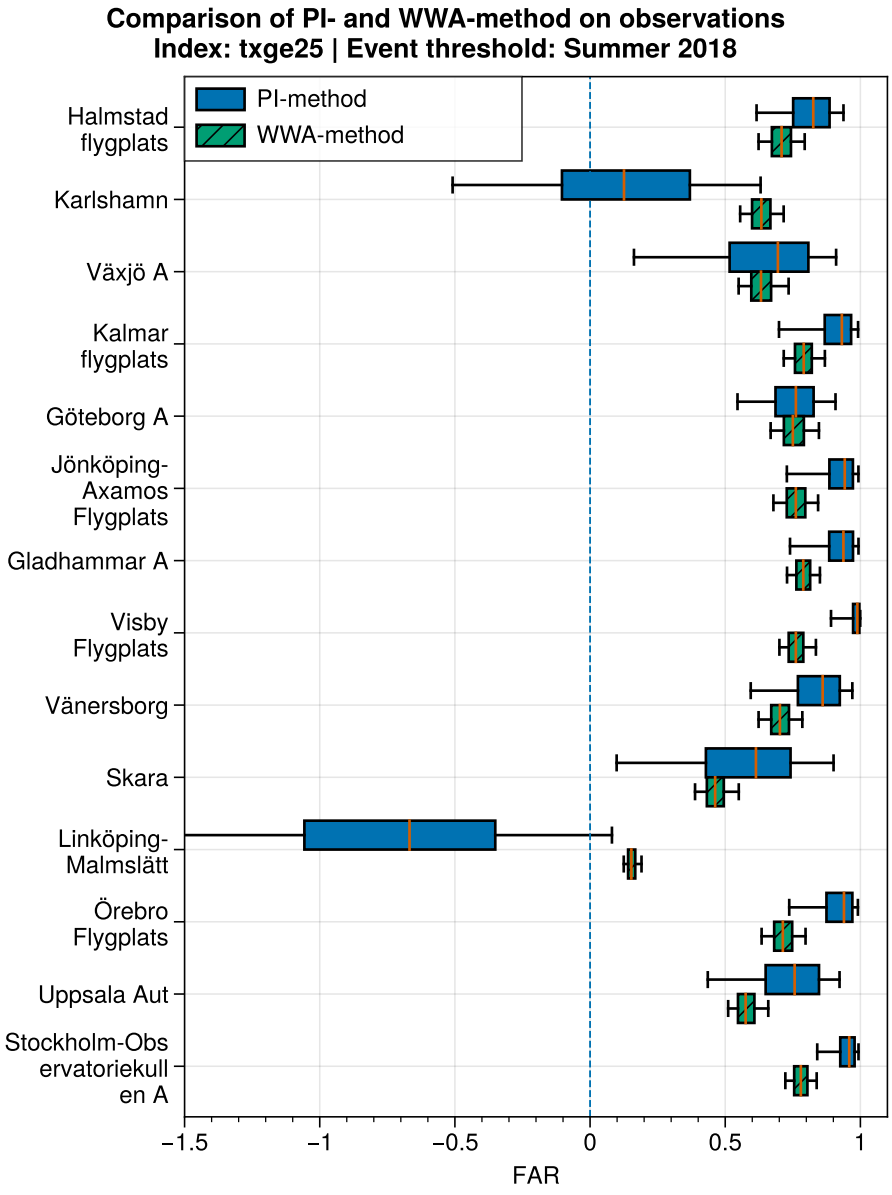

Figure 8. Comparison of FAR distributions for the summer of 2018 from the PI-method and WWA-method applied to txge25 observations of the recent past. The first (blue) of the two bars in every pair shows the FAR distribution of the PI-method, equivalent to what is shown in Fig. 5. The second bar (green, hatched) shows the FAR distribution from applying the WWA-method to the time series of observations of the recent past for each station.

30-years of data, can capture changes in probabilities for a larger scale temperature related event such as the one in the summer of 2018.

For the Gävle event, differences between the FAR distributions for the WWA-method and the PI-method are more varied (Fig. 9). For several stations, the FAR distributions of the WWA- and PI-method generally agree (e.g. Gävle-Åbyggeby, Sveg A, Uppsala, Örebro D). At the other stations, the median FAR from the two methods does not agree, but the uncertainty ranges of the FAR distributions still overlap, mostly due to the large uncertainty in FAR distributions of the PI-method. Furthermore, the much smaller uncertainty in FAR distributions of the WWA-method is a clear indication that the short time periods can lead to over constrained distributions, as discussed above.

~~The~~

For the domain representing the Gävle event, the regression between rx1day (GridClim) and GMST (1989-2018) is relatively strong along, and in proximity to, the coast between 60 and 62°N (Fig. ~~??~~10). Outside this sub-area, the regression is generally weaker and not statistically significant, with no distinguishable spatial patterns. In comparison, the regression between txge25 and GMST in the domain representing the summer of 2018 event exhibits relatively small spatial variations over the domain (Fig. ~~??)over the domain, albeit with fewer significant grid points~~ 10), but with fewer grid points showing a significant regression.

~~For the summer of 2018, shifting the distributions based on observations of the current period leads to an underestimation of FAR compared to the observation-only FAR for most of the stations (Fig. ??). Likely, this is a result of the weak regressioncoefficient between the variable (txge25) and GMST (Fig. A1). There are two stations, Karlshamn and Linköping-Malmslätt, where shifting the current distributions results in a higher estimation of FAR compared to the observations. This anomalous behaviour further supports that these stations suffer from inhomogeneities. For the Gävle event, differences between FAR based on scaling observations of the current period and FAR based on only observations are not as uniform (Fig. ??). At a few stations scaling the distributions of the current period results in a higher FAR compared to observations (e.g. Delsbo A, Härnösand), whereas the scaling results in a lower FAR at e.g. Gävle-Åbyggeby and Uppsala.~~

4 Conclusions

We have conducted two sets of attribution analysis on two notable extreme weather events in Sweden: The warm summer of 2018 and the heavy precipitation event in Gävle 2021. For the ~~initial analysis~~ WWA-method we made use of a number of gridded datasets covering the last decades and assumed that the variable describing the event either shifted, or scaled, with GMST. This allowed us to calculate the probabilities, and their change, for the events ~~during periods~~ from distributions that represent the climate in a pre-industrial period and during the recent past. ~~In the second analysis, we~~ For the PI-method, we instead relied solely on observations to represent the climate during both the pre-industrial ~~(1882-1911) and current (1989-2018)~~ and current periods to retrieve corresponding probabilities. We found the extensive observational record available in Sweden a valuable source of data, that if homogenised could help to further clarify some uncertainties arising from using non-homogenised data.

For the summer of 2018, results ~~using shifting by the relationship to GMST generally agree with the results based on observations when including all stations. However, the adjusted station average, excluding stations likely influenced~~ from the PI-method, excluding stations affected by inhomogeneities, ~~exhibits~~ exhibit a stronger attribution compared to the results of the

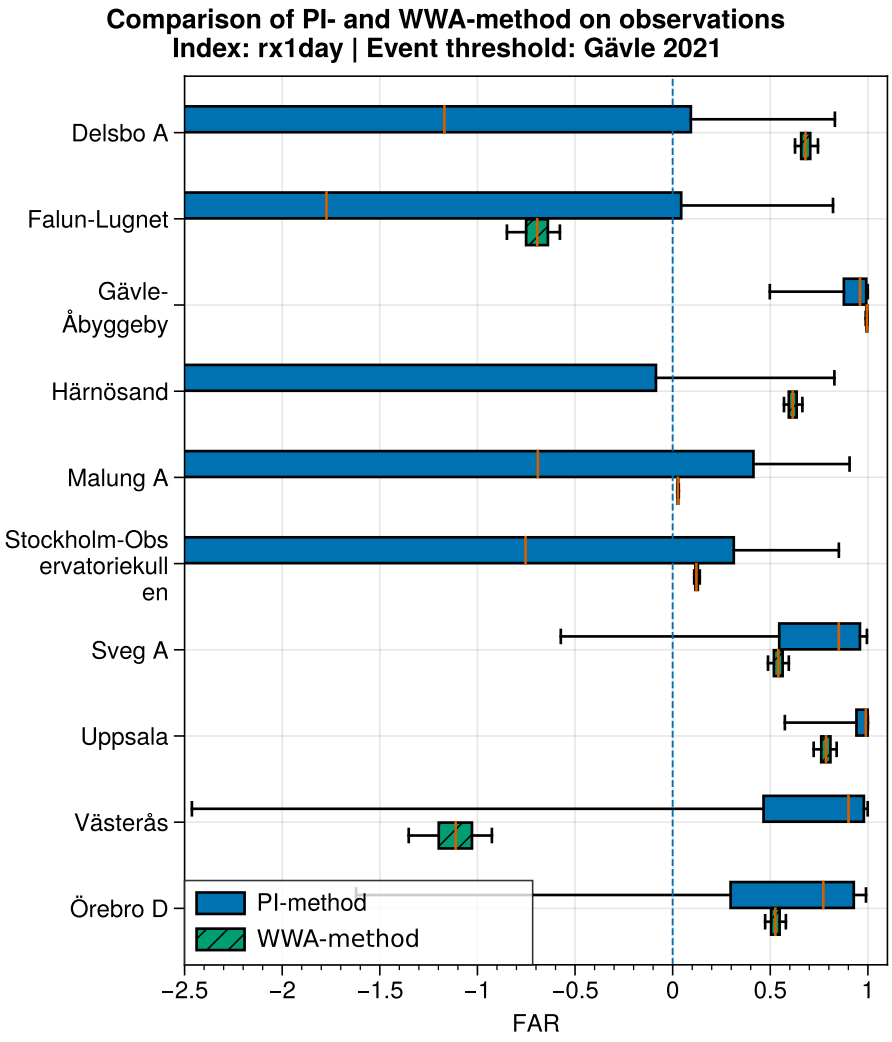

Figure 9. Comparison of FAR distributions for the Gävle 2021 event from the PI-method and WWA-method applied to rx1day observations of the recent past. The first (blue) of the two bars in every pair shows the FAR distribution of the PI-method, equivalent to what is shown in Fig. 7. The second bar (green, hatched) shows the FAR distribution from applying the WWA-method to the time series of observations of the recent past for each station.

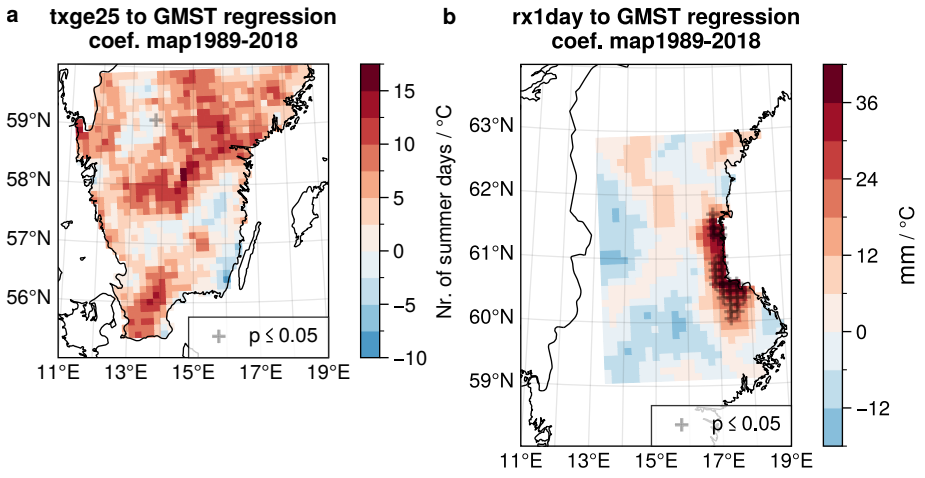

Figure 10. ~~Map of~~ Gridded maps showing the regression coefficients between GMST and GridClim for **a)** the txge25 index over the summer of 2018 domain during 1989-2018, and **b)** the rx1day ~~to GMST regression for GridClim~~index over the Gävle event domain during 1989-2018. Crosses indicate significance at ~~the~~ $p \leq 0.05$~~level~~. For the summer of 2018 domain, the spatial variability is relatively low, with few grid points showing a significant regression. While the Gävle domain shows a cluster of points with a significant regression along the coast between 60° and 62°, the overall spatial variability is greater compared to the summer of 2018.

~~shifted analysis. We also note that with homogenised observations the station-based FAR is likely to increase compared to the current results which are based on unhomogenised data , as the historical data tends to overestimate high temperatures . Overall, for~~ WWA-method. When applied to the ~~case of the summer of 2018, the proposed statistical method from Philip et al. (2020) agrees with the observation-based estimate.~~ station data used in the PI-method, the WWA-method also results in lower values for FAR. The systematic difference between the two approaches using temperature data from the long-term stations indicates that this may be related to the regression between the temperature index (txge25) and GMST. We also note that since high temperatures tend to be overestimated in historical observations, using homogenised observations is likely to result in a higher FAR for heat-wave related extremes using the PI-method. Furthermore, based on these results, we can conclude that 1 out of 2 of every heat wave similar to the summer of 2018 can be attributed to changes in the climate. Alternatively, such heatwaves have become twice as likely due to changes in the climate. When only using station data, the previous statement increases to more than 2 out of 3, and would likely be even higher using homogenised data. ~~Hence, there is a risk that studies that investigate temperature related events, relying solely on shifting following the GMST, underestimate the strength of the attribution.~~

~~For~~ Regarding the precipitation event in Gävle 2021, ~~our results show a fairly good agreement among the gridded datasets, with a median FAR ~ 0.88 and 5th percentile > 0.5, but the variation is large between the stations. A few stations exhibit~~ results from the PI-method are highly variable, making the attribution of the event uncertain. Here, five out of ten stations exhibit a median FAR > 0.5, ~~which is comparable to the gridded analysis, and it is only Gävle-Åbyggeby and Härnösand that exhibit a~~ but only one displays FAR that is significantly above 0. ~~This uncertainty makes it difficult to derive any attribution statements about the precipitation event.~~ On the other hand, except for the ERA5 dataset, there is a fairly good agreement among

the datasets analysed using the WWA-method, and it shows a stronger attribution compared to the PI-method. Applying the WWA-method to the station data used in the PI-method does not reveal any positive, or negative, tendency when comparing the results of the two methods. These large variations within, and between, the two methods make it difficult to draw any conclusions regarding the attribution of the extreme precipitation event in Gävle in 2021.

Comparing the two events, the study indicates that ~~precipitation events~~ a precipitation event like the one in Gävle appears to be more sensitive to the choice of domain ~~. The regression between~~ than a more widespread and uniform heat-wave like the one in the summer of 2018. This agrees with previous findings indicating that extreme precipitation events are more sensitive to the event definition. This is further supported by the regression between extreme temperature and GMST ~~is also~~ being more spatially consistent compared to that between extreme precipitation and GMST. ~~With the high availability of observations in Sweden, a potential improvement to the station-based attribution is to use homogenised data. This would clarify the uncertainties that arise with using non-homogenised observations. However, this is mostly relevant to the investigations of extreme events where long-running observational networks are available.~~ Regarding the more generally applicable ~~regression-based method~~ WWA-method for attribution, future studies should continue to explore how the regional variations in relationships, such as ~~the that between local CC-scaling~~ that between the local Clausius-Clapeyron scaling and GMST, affect the outcome of studies on extreme event attribution.

Code availability. Code used in this analysis is available at https://github.com/Holmgren825/holmgren_kjellstrom_exploring_attribution.

~~Map of the regression coefficients (β) of txge25 to GMST for GridClim. The cross indicates significance at the $p \leq 0.05$ level.~~

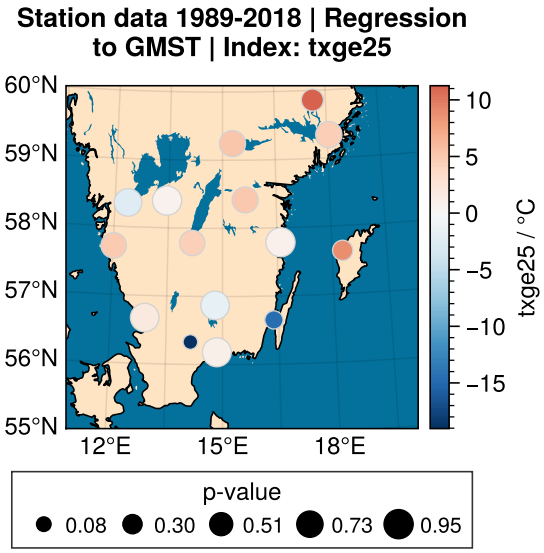

Figure A1. Regression between the index series and GMST at the respective stations. The strength, and sign, of the regression coefficient is indicated by the colour, while the size of the markers indicate the p-value.

Appendix A: Figures

~~Comparison of two sets of FAR distributions. The first of the two bars in every pair is based on the true historic period, equivalent to what is shown in Fig. 7. The second bar shows the results from scaling the distribution of the current climate according to its regression to GMST.~~

~~Trend analysis for the txge25 index. KPSS ≤ 0.05 indicates that a series is non-stationary. ADF ≤ 0.05 indicates that a series is trend stationary.~~

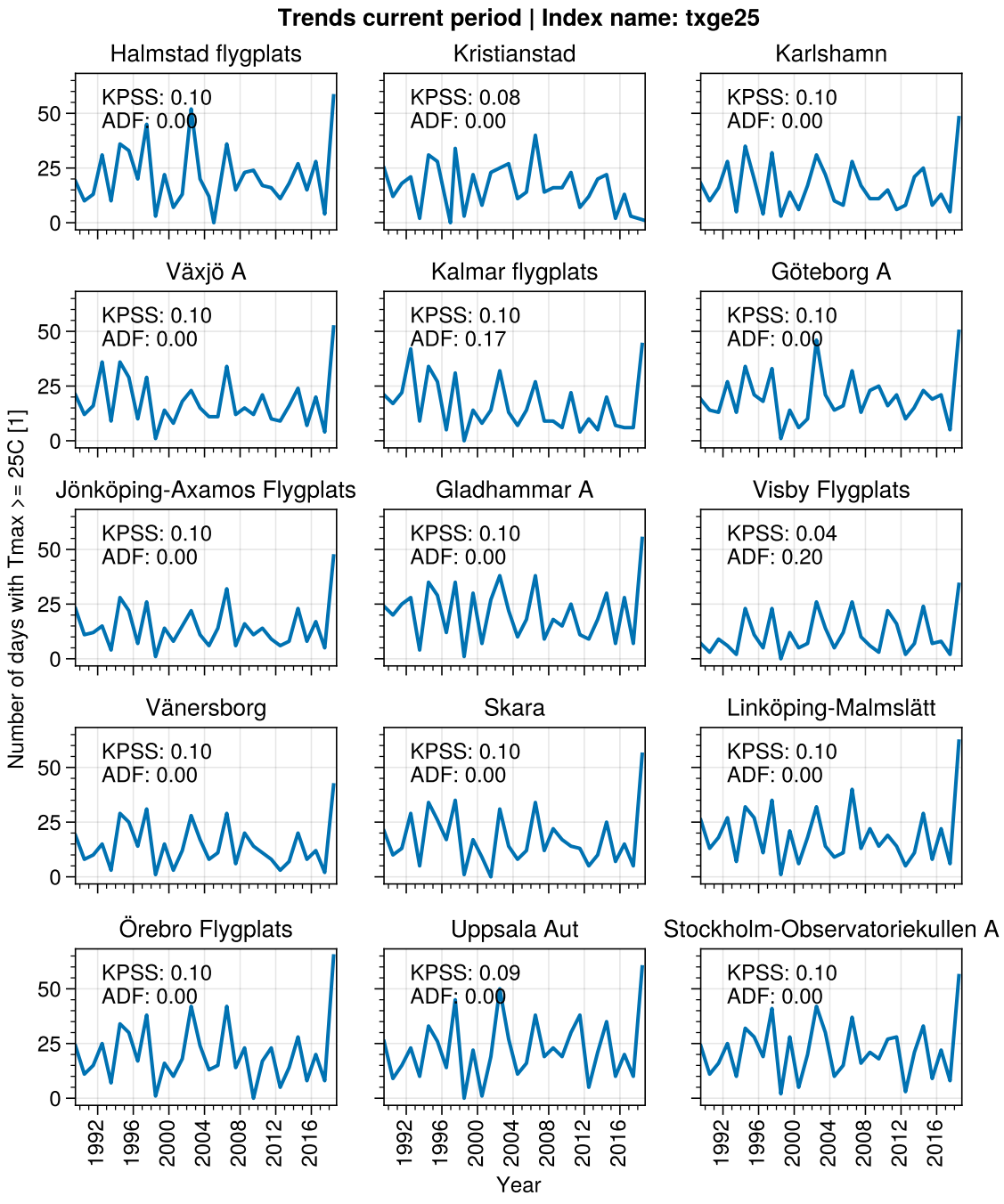

~~stationary.~~

Figure A2. Trend analysis for the txge25 index. KPSS ≤ 0.05 indicates that a series is non-stationary. ADF ≤ 0.05 indicates that a series is trend stationary.

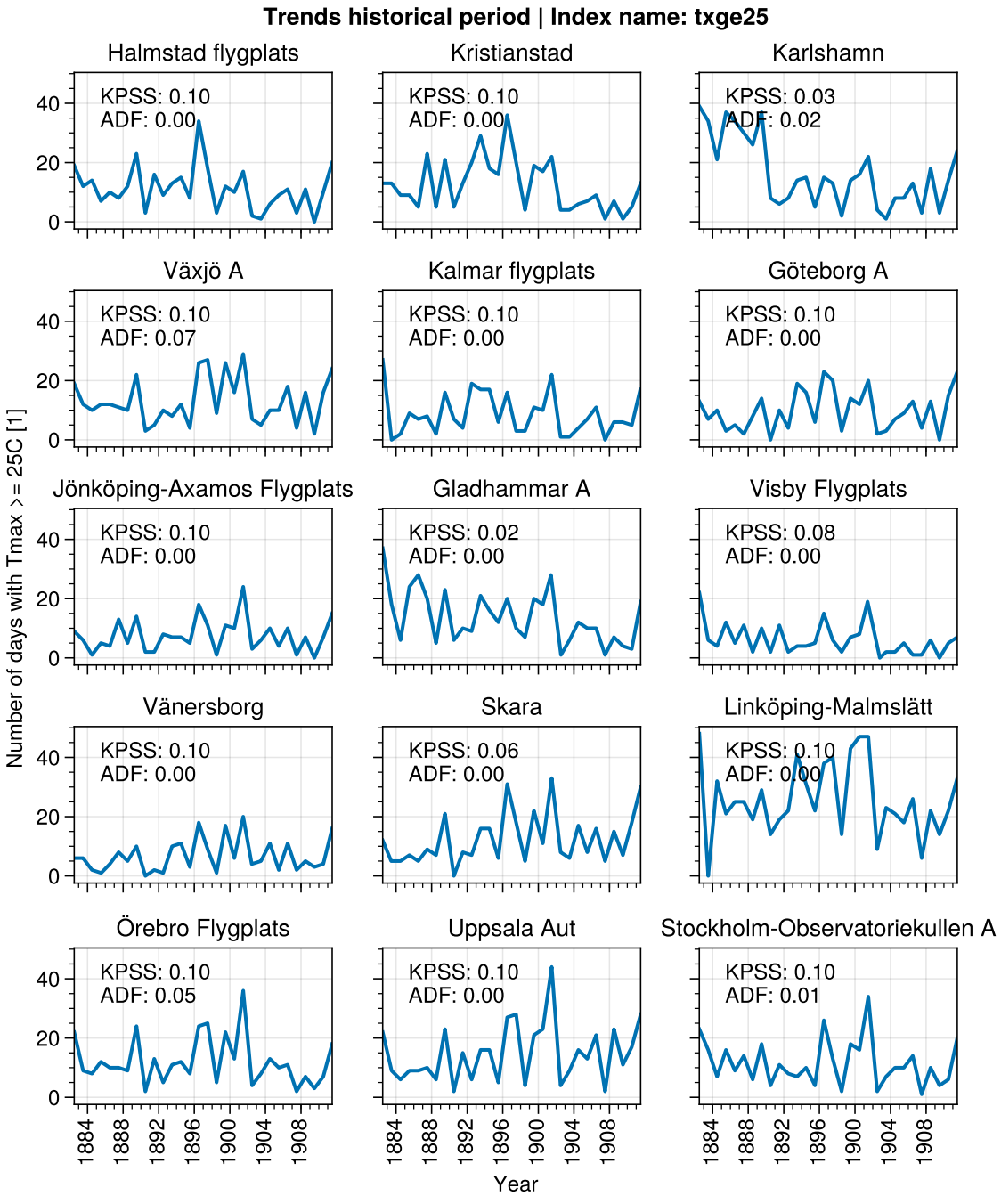

Figure A3. Trend analysis for the ~~rx1day~~ txge25 index. KPSS ≤ 0.05 indicates that a series is non-stationary. ADF ≤ 0.05 indicates that a series is trend stationary.

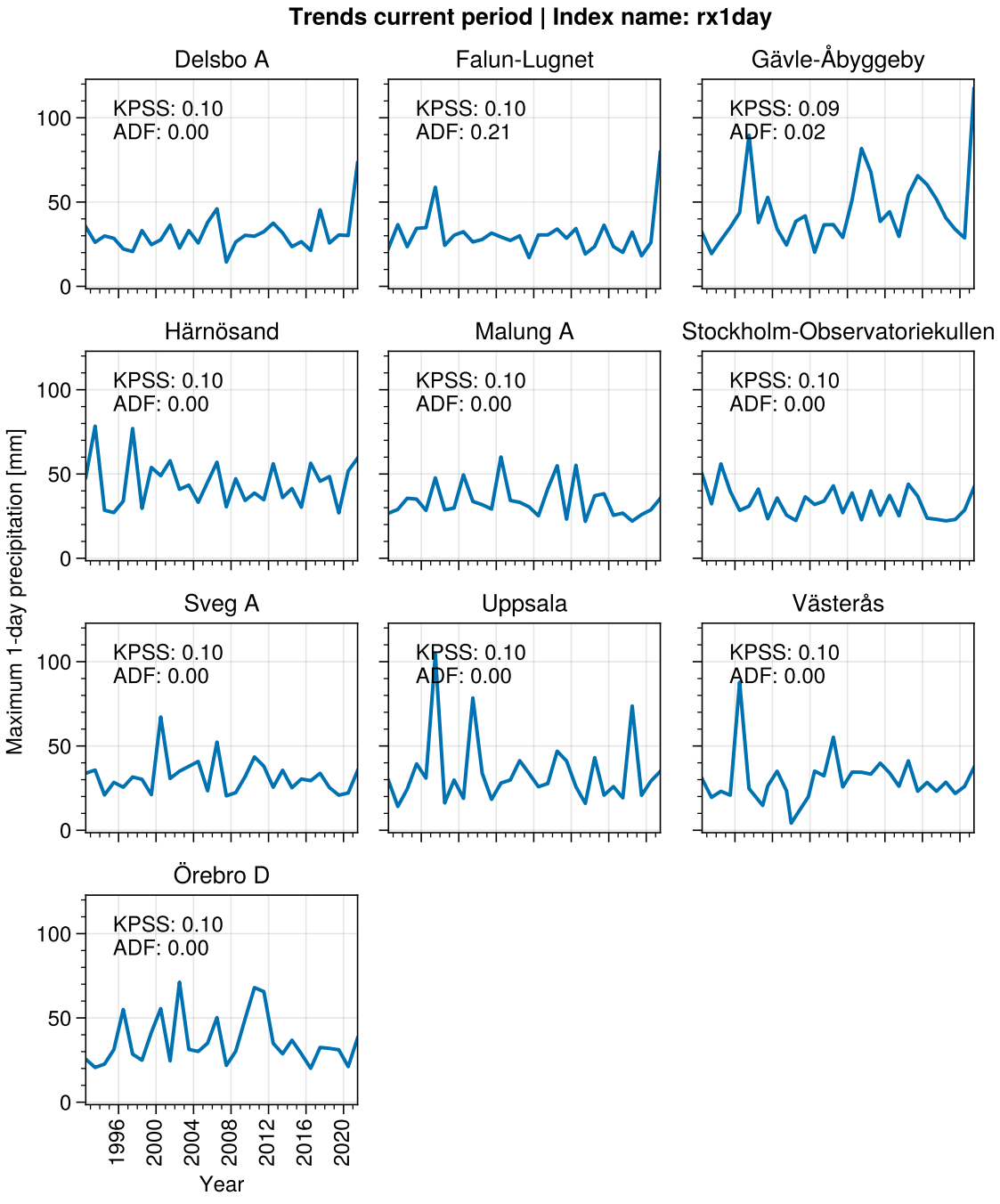

Figure A4. Trend analysis for the rx1day index. KPSS ≤ 0.05 indicates that a series is non-stationary. ADF ≤ 0.05 indicates that a series is trend stationary.

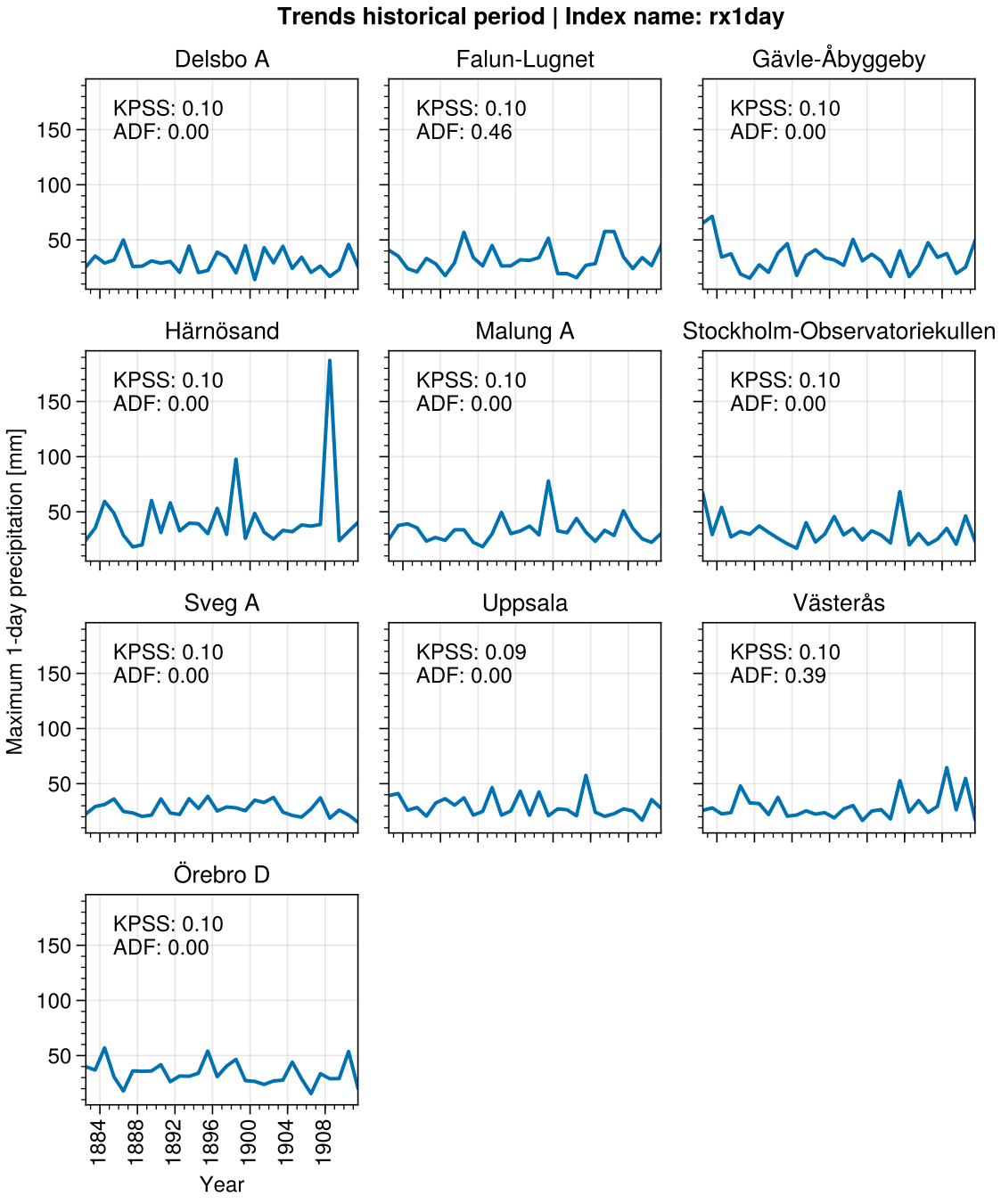

Figure A5. ~~Comparison of two sets of FAR distributions. The first of~~ Trend analysis for the ~~two bars in every pair~~ rx1day index. KPSS < 0.05 indicates that a series is ~~based on the true historic period, equivalent to what~~ non-stationary. ADF < 0.05 indicates that a series is ~~shown in Fig~~trend stationary. ~~5. The second bar shows the results from shifting the distribution of the current climate according to its regression to GMST.~~

Author contributions. EH developed and carried out the analysis, prepared figures, and wrote the article. EK initiated the study, provided comments during the development of the analysis, and assisted in the revision of the article.

Competing interests. The authors have no competing interests to declare.

Acknowledgements. This research was funded by the Swedish Meteorological and Hydrological Institute, specifically the 1:10 government grant Klimatanpassning. We would like to thank the two reviewers for their very valuable comments. Finally, we want to thank Johan Södling for his very appreciated guidance.

References

Alexandersson, H.: Korrektion Av Nederbörd Enligt Enkel Klimatologisk Metodikl, Tech. Rep. 111, SMHI, 2003.

Andersson, S., Bärring, L., Landelius, T., Samuelsson, P., and Schimanke, S.: SMHI Gridded Climatology, 2021.

Bayerisches Landesamt für Umwelt: Das Bayerische Klimaprojektionsensemble Audit Und Ensemblebildung, Tech. rep., Bayerisches Landesamt für Umwelt, 2020.

Berg, P., Bosshard, T., Yang, W., and Zimmermann, K.: MIdASv0.2.1 – MultI-scale Bias AdjuStment, Geoscientific Model Development, 15, 6165–6180, https://doi.org/10.5194/gmd-15-6165-2022, 2022.

Coppola, E., Nogherotto, R., Ciarlo', J. M., Giorgi, F., van Meijgaard, E., Kadygrov, N., Iles, C., Corre, L., Sandstad, M., Somot, S., Nabat, P., Vautard, R., Levavasseur, G., Schwingshackl, C., Sillmann, J., Kjellström, E., Nikulin, G., Aalbers, E., Lenderink, G., Christensen, O. B., Boberg, F., Sørland, S. L., Demory, M.-E., Bülow, K., Teichmann, C., Warrach-Sagi, K., and Wulfmeyer, V.: Assessment of the European Climate Projections as Simulated by the Large EURO-CORDEX Regional and Global Climate Model Ensemble, Journal of Geophysical Research: Atmospheres, 126, https://doi.org/10.1029/2019JD032356, 2021.

Cornes, R. C., van der Schrier, G., van den Besselaar, E. J. M., and Jones, P. D.: An Ensemble Version of the E-OBS Temperature and Precipitation Data Sets, Journal of Geophysical Research: Atmospheres, 123, 9391–9409, https://doi.org/10.1029/2017JD028200, 2018.

Dienst, M., Lindén, J., Engström, E., and Esper, J.: Removing the Relocation Bias from the 155-Year Haparanda Temperature Record in Northern Europe, International Journal of Climatology, 37, 4015–4026, https://doi.org/10.1002/joc.4981, 2017.

Doblas-Reyes, F., Sörensson, A., Almazroui, M., Dosio, A., Gutowski, W., Haarsma, R., Hamdi, R., Hewitson, B., Kwon, W.-T., Lamptey, B., Maraun, D., Stephenson, T., Takayabu, I., Terray, L., Turner, A., and Zuo, Z.: Linking Global to Regional Climate Change, in: Climate Change 2021: The Physical Science Basis. Contribution of Working Group I to the Sixth Assessment Report of the Intergovernmental Panel on Climate Change, edited by Masson-Delmotte, V., Zhai, P., Pirani, A., Connors, S., Péan, C., Berger, S., Caud, N., Chen, Y., Goldfarb, L., Gomis, M., Huang, M., Leitzell, K., Lonnoy, E., Matthews, J., Maycock, T., Waterfield, T., Yelekçi, O., Yu, R., and Zhou, B., pp. 1363–1512, Cambridge University Press, Cambridge, United Kingdom and New York, NY, USA, https://doi.org/10.1017/9781009157896.012, 2021.

Dole, R., Hoerling, M., Perlwitz, J., Eischeid, J., Pegion, P., Zhang, T., Quan, X.-W., Xu, T., and Murray, D.: Was There a Basis for Anticipating the 2010 Russian Heat Wave?, Geophysical Research Letters, 38, https://doi.org/10.1029/2010GL046582, 2011.

Eyring, V., Bony, S., Meehl, G. A., Senior, C. A., Stevens, B., Stouffer, R. J., and Taylor, K. E.: Overview of the Coupled Model Intercomparison Project Phase 6 (CMIP6) Experimental Design and Organization, Geoscientific Model Development, 9, 1937–1958, 2016.

Eyring, V., Gillett, N., Achuta Rao, K., Barimalala, R., Barreiro Parrillo, M., Bellouin, N., Cassou, C., Durack, P., Kosaka, Y., McGregor, S., Min, S., Morgenstern, O., and Sun, Y.: Human Influence on the Climate System, in: Climate Change 2021: The Physical Science Basis. Contribution of Working Group I to the Sixth Assessment Report of the Intergovernmental Panel on Climate Change, edited by Masson-Delmotte, V., Zhai, P., Pirani, A., Connors, S., Péan, C., Berger, S., Caud, N., Chen, Y., Goldfarb, L., Gomis, M., Huang, M., Leitzell, K., Lonnoy, E., Matthews, J., Maycock, T., Waterfield, T., Yelekçi, O., Yu, R., and Zhou, B., pp. 423–552, Cambridge University Press, Cambridge, United Kingdom and New York, NY, USA, https://doi.org/10.1017/9781009157896.005, 2021.

Gulev, S., Thorne, P., Ahn, J., Dentener, F., Domingues, C., Gerland, S., Gong, D., Kaufman, D., Nnamchi, H., Quaas, J., Rivera, J., Sathyendranath, S., Smith, S., Trewin, B., von Schuckmann, K., and Vose, R.: Changing State of the Climate System, in: Climate Change 2021: The Physical Science Basis. Contribution of Working Group I to the Sixth Assessment Report of the Intergovernmental Panel on Climate Change, edited by Masson-Delmotte, V., Zhai, P., Pirani, A., Connors, S., Péan, C., Berger, S., Caud, N., Chen, Y., Goldfarb, L., Gomis,

M., Huang, M., Leitzell, K., Lonnoy, E., Matthews, J., Maycock, T., Waterfield, T., Yelekçi, O., Yu, R., and Zhou, B., pp. 287–422, Cambridge University Press, Cambridge, United Kingdom and New York, NY, USA, https://doi.org/10.1017/9781009157896.004, 2021.

Hansen, J., Ruedy, R., Sato, M., and Lo, K.: Global Surface Temperature Change, Reviews of Geophysics, 48, https://doi.org/10.1029/2010RG000345, 2010.

Herring, S. C., Christidis, N., Hoell, A., and Stott, P. A.: Explaining Extreme Events of 2020 from a Climate Perspective, Bulletin of the American Meteorological Society, 103, S1–S129, https://doi.org/10.1175/BAMS-ExplainingExtremeEvents2020.1, 2022.

Hersbach, H., Bell, B., Berrisford, P., Hirahara, S., Horányi, A., Muñoz-Sabater, J., Nicolas, J., Peubey, C., Radu, R., Schepers, D., Simmons, A., Soci, C., Abdalla, S., Abellan, X., Balsamo, G., Bechtold, P., Biavati, G., Bidlot, J., Bonavita, M., De Chiara, G., Dahlgren, P., Dee, D., Diamantakis, M., Dragani, R., Flemming, J., Forbes, R., Fuentes, M., Geer, A., Haimberger, L., Healy, S., Hogan, R. J., Hólm, E., Janisková, M., Keeley, S., Laloyaux, P., Lopez, P., Lupu, C., Radnoti, G., de Rosnay, P., Rozum, I., Vamborg, F., Villaume, S., and Thépaut, J.-N.: The ERA5 Global Reanalysis, Quarterly Journal of the Royal Meteorological Society, 146, 1999–2049, https://doi.org/10.1002/qj.3803, 2020.

Hoerling, M., Kumar, A., Dole, R., Nielsen-Gammon, J. W., Eischeid, J., Perlwitz, J., Quan, X.-W., Zhang, T., Pegion, P., and Chen, M.: Anatomy of an Extreme Event, Journal of Climate, 26, 2811–2832, https://doi.org/10.1175/JCLI-D-12-00270.1, 2013.

Holland, G. and Bruyère, C. L.: Recent Intense Hurricane Response to Global Climate Change, Climate Dynamics, 42, 617–627, https://doi.org/10.1007/s00382-013-1713-0, 2014.

IPCC: Climate Change 2021: The Physical Science Basis. Contribution of Working Group I to the Sixth Assessment Report of the Intergovernmental Panel on Climate Change, vol. In Press, Cambridge University Press, Cambridge, United Kingdom and New York, NY, USA, https://doi.org/10.1017/9781009157896, 2021.

Jacob, D., Petersen, J., Eggert, B., Alias, A., Christensen, O. B., Bouwer, L. M., Braun, A., Colette, A., Déqué, M., Georgievski, G., Georgopoulou, E., Gobiet, A., Menut, L., Nikulin, G., Haensler, A., Hempelmann, N., Jones, C., Keuler, K., Kovats, S., Kröner, N., Kotlarski, S., Kriegsmann, A., Martin, E., van Meijgaard, E., Moseley, C., Pfeifer, S., Preuschmann, S., Radermacher, C., Radtke, K., Rechid, D., Rounsevell, M., Samuelsson, P., Somot, S., Soussana, J.-F., Teichmann, C., Valentini, R., Vautard, R., Weber, B., and Yiou, P.: EURO-CORDEX: New High-Resolution Climate Change Projections for European Impact Research, Regional Environmental Change, 14, 563–578, https://doi.org/10.1007/s10113-013-0499-2, 2014.

Joelsson, L. M. T., Engström, E., and Kjellström, E.: Homogenization of Swedish Mean Monthly Temperature Series 1860–2021, International Journal of Climatology, 43, 1079–1093, https://doi.org/10.1002/joc.7881, 2022.

Johansson, B.: Areal Precipitation and Temperature in the Swedish Mountains: An Evaluation from a Hydrological Perspective, Hydrology Research, 31, 207–228, https://doi.org/10.2166/nh.2000.0013, 2000.

Johansson, B. and Chen, D.: The Influence of Wind and Topography on Precipitation Distribution in Sweden: Statistical Analysis and Modelling, International Journal of Climatology: A Journal of the Royal Meteorological Society, 23, 1523–1535, 2003.

Johansson, B. and Chen, D.: Estimation of Areal Precipitation for Runoff Modelling Using Wind Data: A Case Study in Sweden, Climate Research, 29, 53–61, 2005.

Jones, C., Giorgi, F., and Asrar, G.: The Coordinated Regional Downscaling Experiment: CORDEX, An International Downscaling Link to CMIP5, CLIVAR Exchanges, 16, 34–40, 2011.

Kjellström, E., Andersson, L., Arneborg, L., Berg, P., Capell, R., Fredriksson, S., Hieronymus, M., Jönsson, A., Lindström, L., and Strandberg, G.: Klimatinformation som stöd för samhällets klimatanpassningsarbete, Tech. Rep. 64, SMHI, 2022.

Lavers, D. A., Simmons, A., Vamborg, F., and Rodwell, M. J.: An Evaluation of ERA5 Precipitation for Climate Monitoring, Quarterly Journal of the Royal Meteorological Society, 148, 3152–3165, https://doi.org/10.1002/qj.4351, 2022.

Leach, N., Li, S., Sparrow, S., Van Oldenborgh, G. J., Lott, F. C., Weisheimer, A., and Allen, M. R.: Anthropogenic Influence on the 2018 Summer Warm Spell in Europe: The Impact of Different Spatio-Temporal Scales, Bulletin of the American Meteorological Society, 101, 2020.

Olsson, L., Thorén, H., Harnesk, D., and Persson, J.: Ethics of Probabilistic Extreme Event Attribution in Climate Change Science: A Critique, Earth's Future, 10, e2021EF002 258, https://doi.org/10.1029/2021EF002258, 2022.

Otto, F. E. L., Massey, N., van Oldenborgh, G. J., Jones, R. G., and Allen, M. R.: Reconciling Two Approaches to Attribution of the 2010 Russian Heat Wave, Geophysical Research Letters, 39, https://doi.org/10.1029/2011GL050422, 2012.

Parker, H. R., Cornforth, R. J., Boyd, E., James, R., Otto, F. E. L., and Allen, M. R.: Implications of Event Attribution for Loss and Damage Policy, Weather, 70, 268–273, https://doi.org/10.1002/wea.2542, 2015.

Philip, S., Kew, S., van Oldenborgh, G. J., Otto, F., Vautard, R., van der Wiel, K., King, A., Lott, F., Arrighi, J., Singh, R., and van Aalst, M.: A Protocol for Probabilistic Extreme Event Attribution Analyses, Advances in Statistical Climatology, Meteorology and Oceanography, 6, 177–203, https://doi.org/10.5194/ascmo-6-177-2020, 2020.

Rahmstorf, S. and Coumou, D.: Increase of Extreme Events in a Warming World, Proceedings of the National Academy of Sciences, 108, 17 905–17 909, https://doi.org/10.1073/pnas.1101766108, 2011.

Rizwan, A. M., Dennis, L. Y. C., and Liu, C.: A Review on the Generation, Determination and Mitigation of Urban Heat Island, Journal of Environmental Sciences, 20, 120–128, https://doi.org/10.1016/S1001-0742(08)60019-4, 2008.

Seneviratne, S., Zhang, X., Adnan, M., Badi, W., Dereczynski, C., Di Luca, A., Ghosh, S., Iskandar, I., Kossin, J., Lewis, S., Otto, F., Pinto, I., Satoh, M., Vicente-Serrano, S., Wehner, M., and Zhou, B.: Weather and Climate Extreme Events in a Changing Climate, in: Climate Change 2021: The Physical Science Basis. Contribution of Working Group I to the Sixth Assessment Report of the Intergovernmental Panel on Climate Change, edited by Masson-Delmotte, V., Zhai, P., Pirani, A., Connors, S., Péan, C., Berger, S., Caud, N., Chen, Y., Goldfarb, L., Gomis, M., Huang, M., Leitzell, K., Lonnoy, E., Matthews, J., Maycock, T., Waterfield, T., Yelekçi, O., Yu, R., and Zhou, B., pp. 1513–1766, Cambridge University Press, Cambridge, United Kingdom and New York, NY, USA, https://doi.org/10.1017/9781009157896.013, 2021.

Stott, P. A., Christidis, N., Otto, F. E. L., Sun, Y., Vanderlinden, J.-P., van Oldenborgh, G. J., Vautard, R., von Storch, H., Walton, P., Yiou, P., and Zwiers, F. W.: Attribution of Extreme Weather and Climate-Related Events, WIREs Climate Change, 7, 23–41, https://doi.org/10.1002/wcc.380, 2016.

Trenberth, K. E.: Changes in Precipitation with Climate Change, Climate Research, 47, 123–138, https://doi.org/10.3354/cr00953, 2011.

Tuomenvirta, H.: Homogeneity Adjustments of Temperature and Precipitation Series—Finnish and Nordic Data, International Journal of Climatology, 21, 495–506, https://doi.org/10.1002/joc.616, 2001.

van Oldenborgh, G. J., van der Wiel, K., Kew, S., Philip, S., Otto, F., Vautard, R., King, A., Lott, F., Arrighi, J., Singh, R., and van Aalst, M.: Pathways and Pitfalls in Extreme Event Attribution, Climatic Change, 166, 13, https://doi.org/10.1007/s10584-021-03071-7, 2021.

Virtanen, P., Gommers, R., Oliphant, T. E., Haberland, M., Reddy, T., Cournapeau, D., Burovski, E., Peterson, P., Weckesser, W., Bright, J., van der Walt, S. J., Brett, M., Wilson, J., Millman, K. J., Mayorov, N., Nelson, A. R. J., Jones, E., Kern, R., Larson, E., Carey, C. J., Polat, İ., Feng, Y., Moore, E. W., VanderPlas, J., Laxalde, D., Perktold, J., Cimrman, R., Henriksen, I., Quintero, E. A., Harris, C. R., Archibald, A. M., Ribeiro, A. H., Pedregosa, F., and van Mulbregt, P.: SciPy 1.0: Fundamental Algorithms for Scientific Computing in Python, Nature Methods, 17, 261–272, https://doi.org/10.1038/s41592-019-0686-2, 2020.

Wilcke, R. A. I., Kjellström, E., Lin, C., Matei, D., Moberg, A., and Tyrlis, E.: The Extremely Warm Summer of 2018 in Sweden – Set in a Historical Context, Earth System Dynamics, 11, 1107–1121, https://doi.org/10.5194/esd-11-1107-2020, 2020.

Yiou, P., Cattiaux, J., Faranda, D., Kadygrov, N., Jézéquel, A., Naveau, P., Ribes, A., Robin, Y., Thao, S., and van Oldenborgh, G. J.: Analyses of the Northern European Summer Heatwave of 2018, Bulletin of the American Meteorological Society, 101, S35–S40, 2020.

Zimmermann, K., Bärring, L., Löw, J., and Nilsson, C.: Climix—a Flexible Suite for the Calculation of Climate Indices, 2023.